PAPER

Stepwise ammonium enrichment using selective battery electrodes†

Moon Son, [iD] [a] Eric Kolvek, [iD] [b] Taeyoung Kim, [iD] [c] Wulin Yang, [iD] [a]
Johannes S. Vrouwenvelder, [d] Christopher A. Gorski [iD] [a] and Bruce E. Logan [iD] *[a]

Ammonium is typically removed from treated wastewaters before discharge by converting it to nitrogen gas, but its capture and reuse could provide a new strategy for energy recovery at treatment plants. A three-stage electrochemical approach was developed here to selectively remove and concentrate ammonium derived from wastewater. Each stage contained a battery electrode deionization (BDI) cell containing two copper hexacyanoferrate (CuHCF) electrodes separated into two channels using an anion exchange membrane. Through application of a low applied voltage (0.3 V) in each of the three stages, ammonium was concentrated greater than 6 times, from 5 to 32 mM (90 to 576 mg L^{-1}), with minimal changes in the concentration of other cations (Na^+, K^+, Mg^{2+}, and Ca^{2+}) present in the water due to the high ammonium ion selectivity of CuHCF electrodes under these operating conditions. The cumulative energy use for the three-stage process was only 2.0 kW h per kg-N, compared to the 14 kW h per kg-N that would be needed to manufacture this amount of ammonium from nitrogen gas. Nitrogen recovery methods such as these will be needed to further transform used water plants into more effective resource recovery treatment plants.

Water impact

Ammonia production is an energy intensive process, so the ammonium ions in wastewaters can be a valuable resource for energy recovery. In this study, it was demonstrated that by using a series of electrochemical cells containing battery electrodes that ammonium could be selectively removed with a low energy demand, and then further concentrated (>6 times) for more efficient ammonium recovery.

1. Introduction

Used waters from homes and businesses, traditionally called wastewaters, are sent to treatment plants to remove organic matter as well as nutrients that can lead to the eutrophication of receiving water bodies.[1–4] However, these treatment plants are now being viewed as resource recovery plants, as treatment can provide opportunities to capture energy from oxidation of the organic matter, biosolids that can be used for agriculture, and nutrients for reuse as

fertilizer.[5–8] Ammonium nitrogen is especially valuable due to the high energy needed to produce it using the Haber Bosch process (14 kW h per kg-N),[9] but it is not currently recovered at these treatment plants. Ammonium in water is usually removed in conventional treatment processes through conversion to N_2 gas through nitrification–denitrification processes.[10,11] To reduce energy consumption at typical activated sludge wastewater treatment plants of ~0.6 kW h m^{-3} of treated water,[12] new anaerobic treatment technologies are being investigated as they avoid the need for wastewater aeration. However, fully anaerobic treatment processes cannot accomplish nitrification for ammonium removal because the reaction requires molecular oxygen. Thus, effective and economical methods are needed to remove and recover ammonium from both conventional and new anaerobic treatment technologies.

Economical ammonium nitrogen removal from treated used waters is especially challenging due to its low concentration in received water (<2 to 5 mM; <28 to 70 mg L^{-1} as NH_4^+-N).[13–15] One way to improve economic recovery of ammonium is to concentrate it before using other

[a] *Department of Civil and Environmental Engineering, The Pennsylvania State University, University Park, PA 16802, USA. E-mail: blogan@psu.edu;*
Tel: +1 814 863 7908
[b] *Department of Chemical Engineering, The Pennsylvania State University, University Park, PA 16802, USA*
[c] *Department of Chemical and Biomolecular Engineering, and Institute for a Sustainable Environment, Clarkson University, Potsdam, NY 13699, USA*
[d] *Water Desalination and Reuse Center (WDRC), Division of Biological and Environmental Science and Engineering (BESE), King Abdullah University of Science and Technology (KAUST), Thuwal 23955-6900, Saudi Arabia*
† Electronic supplementary information (ESI) available. See DOI: 10.1039/d0ew00010h

This journal is © The Royal Society of Chemistry 2020

Environ. Sci.: Water Res. Technol., 2020, **6**, 1649–1657 | **1649**

conventional methods to extract ammonium from the water. Once concentrated, ammonium can be removed by conversion into volatile ammonia by raising the solution pH, followed by air stripping and NH_3 scrubbers to form useful fertilizers, such as $(NH_4)_2SO_4$.[16–18] Ion exchange (IE) and reverse osmosis (RO) have been investigated to generate ammonia-rich solutions.[19–21] However, IE requires a complex regeneration process and it generates a secondary waste.[22] RO can also be used although like these other processes they are not highly selective for ammonium ion removal compared to other cations, and it has relatively low water recovery ratio.[23] One strategy for concentrating ammonium is to use electrochemical cells. Cells that rely on the capacitance processes to remove ions can be used to concentrate ammonium, but they do not effectively select for ammonium over other ions as all ions are removed and concentrated near the electrode surface (i.e., >90% of ammonium removal with >60% of sodium removal).[19,24–28] Thus, capacitive-based electrode systems showed relatively high energy demands of 4.4–21.7 kW h per kg-N for ammonium removal (initial NH_4^+ of ~3 mM).[29–31] Intercalation electrodes[32–36] are a compelling solution to this problem because, unlike capacitive electrodes, they can selectively remove the target cations[32–35] or anions.[36] A new approach was recently developed that was selective for ammonium compared to Na^+ ions (>90%),[35] and had an energy consumption (1.5 kW h per kg-N with 0.2 V applied) that was only 7 to 17% of that needed in other electrochemical systems such as flow-electrode capacitive deionization (CDI) or electrodialysis (ED).[17,30] This battery electrode deionization (BDI) process used intercalation electrodes of a well-known perovskite-like cubic crystal structure containing copper hexacyanoferrate (CuHCF).[37] The CuHCF electrode intercalates cations within a cage-like structure which reduces Fe^{III} to Fe^{II}.[37] The selective removal of ammonium ions was based on their relatively smaller hydrated radius (3.3 Å) and faster diffusivity than sodium ions (3.6 Å) into interstitial sites (estimated diameters of 3.2 to 4.6 Å).[37–41] In a BDI or CDI system, typically 50% of the water is treated and the other half of the flow is released as a concentrated stream. While this flow scheme may be useful for producing desalinated water, ammonia recovery from the concentrated stream requires further concentration to reduce the volume of the water containing the ammonia in order to make the process practical.

A new approach for concentrating ammonium is proposed here based on stepwise concentration of ammonium in wastewater using a multiple-staged electrochemical cell system (Fig. 1). Previous BDI systems have examined only the production of lower salinity or lower ammonium treated water streams, but have not addressed the fate of the concentrated solution. In the staged process proposed here the concentrated solution from the first stage, containing concentrated ammonia, is sent to a second BDI stage. The treated water from this second stage is then recycled back to the first stage influent, and the concentrated stream is sent to a third stage (Fig. 1). As a result of this recycling process, overall 75% of the water is released as treated water, with ammonia concentrated into 25% of the final concentrated
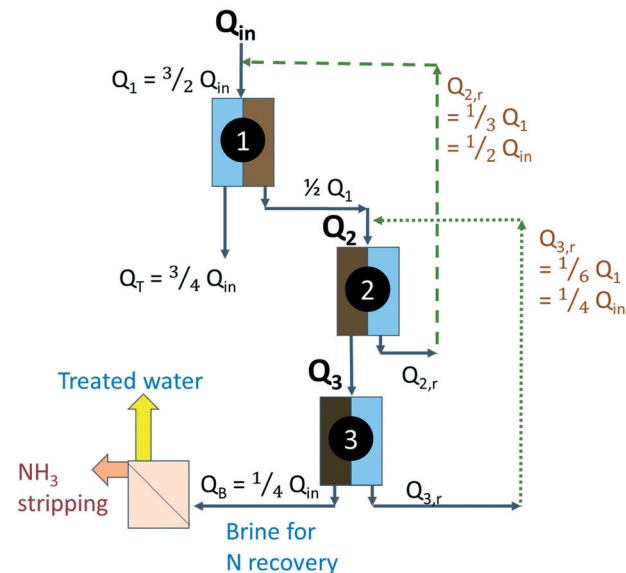

Fig. 1 Example of the flow in a three-stage BDI process, with 50% of the flow in each effluent stream, showing recycle streams being used to concentrate the ammonium ions into 25% of the overall flow, with 75% of the total influent water treated to remove ammonium.

solution. The concentrated stream can be further concentrated using additional BDI stages or other processes, for example by adjusting the concentrated solution flows to be smaller than that of the treated flow.[35] A final process such as ammonia stripping or adjusting solution pH producing a highly concentrated ammonium product suitable for fertilizer such as ammonium sulfate or magnesium ammonium phosphate hexahydrate.[16–18,42–44]

To examine the extent of ammonium concentration that might be possible in such a staged process, a synthetic solution containing ammonium and sodium ions as cations was first examined in a three-stage simulated process, as sodium is the most abundant cation in typical wastewater. Following these tests, a synthetic wastewater containing a more complete array of cations (Na^+, NH_4^+, K^+, Mg^{2+}, and Ca^{2+}) was examined in order to provide results more representative of actual domestic wastewaters. For simplicity of experiment design, we did not conduct tests using actual wastewaters as our previous tests using BDI showed that there was no appreciable difference in performance between synthetic and actual wastewaters if they had the same ionic composition.[35] The energy used for the separation of ammonium here was evaluated based on the applied voltage and current in each cycle.

2. Materials and methods

2.1. Battery electrode preparation

CuHCF powder was synthesized using a co-precipitation method as previously reported.[35,45–47] Briefly, 80 mL of 0.1 M $Cu(NO_3)_2$ (Sigma-Aldrich) and 80 mL of 0.05 M $K_3[Fe(CN)_6]$ (J. T. Baker) were simultaneously added (flow rate of 0.5 mL

1650 | Environ. Sci.: Water Res. Technol., 2020, 6, 1649–1657

This journal is © The Royal Society of Chemistry 2020

min^{-1}) to 40 mL of deionized (DI) water with vigorous stirring (~300 rpm). The precipitates were washed four times by centrifugation at 7800 × g for 10 min at 20 °C (Thermo Scientific, Sorvall LYNX 4000) using deionized water, and dried overnight in a vacuum oven at 70 °C. The solid precipitates were then gently milled to produce the CuHCF powder used to fabricate the electrodes on a carbon cloth (1071HCB, AvCarb Material Solutions). A slurry composed of CuHCF (80 wt%), carbon black (10 wt%, Vulcan XC72R, Cabot), and polyvinyledenefluoride (10 wt%, Kynar HSV 900, Arkema Inc) in 1-methyl-2-pyrrolidinone (Sigma-Aldrich) was loaded onto the carbon cloth using a pipette. The electrode was heated at 70 °C for 1 h using a hot plate to remove solvent, and then dried overnight at 70 °C in a vacuum oven.

2.2. Electrochemical cell construction

The flow cell contained two CuHCF electrodes separated by an AEM (Selemion AMV, Asahi Glass, Japan) (Fig. 2a and S1†) fit into cylindrical chambers (diameter = 30 mm and area = 7 cm^2) containing fabric spacers (Sefar Nitex 03-200/54, thickness = 120 μm). Flow entered one side of the chamber and exited on the far side of each chamber, with co-current flow directions. Graphite foil was used as current collector for the carbon cloth electrode, with rubber gaskets were placed between each component in order to prevent leakage

of solution. The conductivity of the solution leaving each chamber was monitored using a flow-through conductivity meter (ET908, eDAQ, Australia). Before the electrodes were placed into the test cell, the potential of the two CuHCF electrodes were adjusted to 0.6 and 1.0 V (*versus* Ag/AgCl in 3 M NaCl. Working electrolyte was 1 M NH$_4$Cl) in a separate 3-electrode cell (~2 cm long by ~3 cm in diameter) containing working (CuHCF), counter (activated carbon and carbon black), and reference electrodes (Ag/AgCl in 3 M NaCl). This preconditioning of the electrodes by setting the voltage to 0.6 and 1.0 V was conducted to maximize NH$_4^+$ removal since that is an optimum voltage window for NH$_4^+$ compared to other cations (Na$^+$, K$^+$, Mg^{2+}, and Ca^{2+}) based on cyclic voltammograms collected in 1 M solutions.[35] Applied voltages of either 0.1 V or 0.3 V were chosen as these applied voltages showed excellent NH$_4^+$ removals of either 65.2 ± 4.0% (0.1 V) or 94.3 ± 0.4% (0.3 V) in a previous study.[35]

2.3. Ammonium enrichment and removal tests

Electrochemical removal of cations by the CuHCF can be expressed as

$$Y^+Cu[Fe^{III}(CN)_6] + xY^+ + xe^-$$
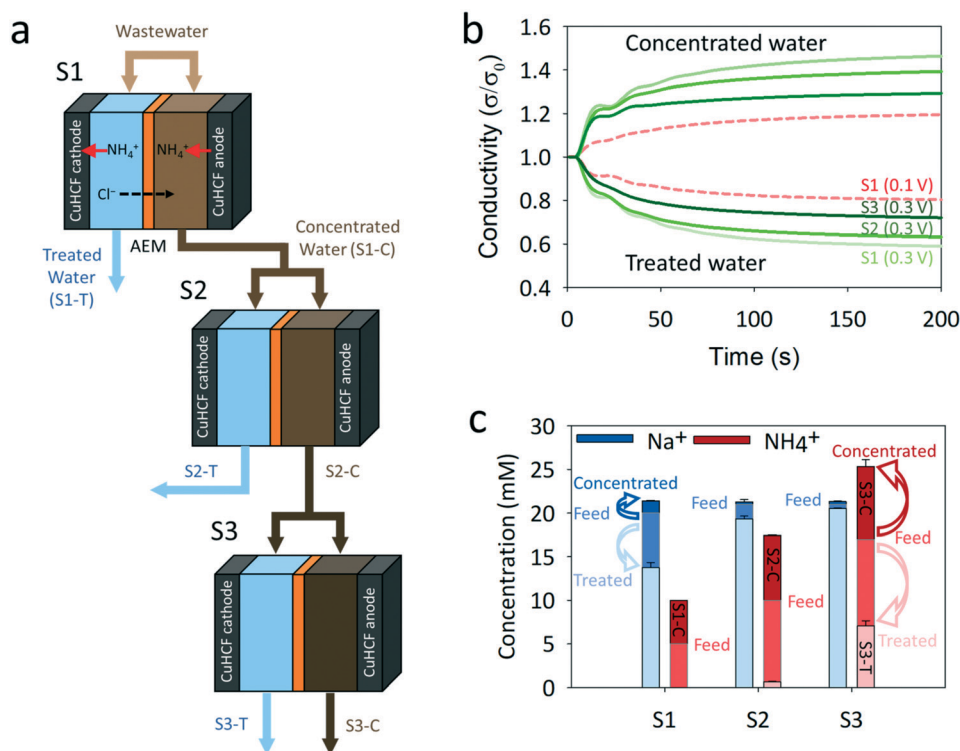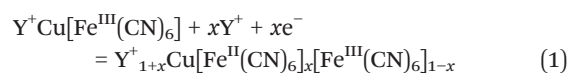$$= Y^+_{1+x}Cu[Fe^{II}(CN)_6]_x[Fe^{III}(CN)_6]_{1-x} \qquad (1)$$

Fig. 2 (a) Schematic of three-stage electrochemical cell using selective battery electrodes, copper hexacyanoferrate (CuHCF), in two channels divided by an anion exchange membrane (AEM). (b) Conductivity profiles of treated and concentrated waters. Concentration of the feed waters was varied depending on the effluent concentration of the previous stage (S1: 20 mM NaCl and 5 mM NH$_4$Cl, S2: 21 mM NaCl and 10 mM NH$_4$Cl, and S3: 21 mM NaCl and 17 mM NH$_4$Cl). (c) Concentration of the feed, treated, and concentrated waters of Na$^+$ and NH$_4^+$ over three stages at an applied voltage of 0.3 and −0.3 V. Error bars show the range from at least duplicate experiments.

This journal is © The Royal Society of Chemistry 2020

Environ. Sci.: Water Res. Technol., 2020, **6**, 1649–1657 | **1651**

where Y stands for cations such as NH_4^+, Na^+, and K^+. The CuHCF electrode can take up the cations into interstitial sites (Fig. S2†). During charging, as cations are removed from the synthesis water, anions migrate through the AEM to the opposite solution (Fig. 2a). Cations from the previous cycle that were stored in the electrode then move out of the electrode into the concentrate stream as well. For a multiple stage system, the concentrated stream of the previous stage becomes the feed solution of the next stage. For instance, concentrated stream of the first stage (S1-C) was a feed solution for the second stage (Fig. 2a).

To test this three-stage concept, a synthetic solution containing 20 mM NaCl and 5 mM NH_4Cl was used as a feed solution for the first stage, as the Na^+ ion concentration is usually much larger than that of the NH_4^+ ions in treated used waters.[35] The flow cell was fed by a fresh feed solution at a flow rate of 4 mL min^{-1} until the effluent concentration was stable based on its conductivity.[35] A volume of fluid (~1 mL) was then recycled through the chamber using an external loop for a single cycle, where alternating voltages of 0.1/−0.1 V or 0.3/−0.3 V were applied to the electrodes for 200 s using a potentiostat (VMP3, Bio-Logic). For the second and third cycles, fresh solutions were used that were made with a composition identical to the effluent of the concentrated solution generated when 0.3/−0.3 V were used in the previous stage due to the improved NH_4^+ concentration at the higher applied voltage.

The concentrations of Na^+ and NH_4^+ were analyzed using ion chromatography (ICS-1100, Dionex) using Dionex IonPac CS16 (5 × 250 mm) and CG 16 (5 × 50 mm) columns. Methanesulfonic acid (30 mM, Sigma-Aldrich) was used as the eluent at a flow rate of 1.0 mL min^{-1}.

2.4. Calculations

The selectivity to the ammonium (S_A) in each stage was calculated as

$$S_A = \frac{C_A}{C_S} \tag{2}$$

where C_A is the ammonium removed, and C_S is the sodium ions removed.

The cumulative charge (C_e, μmol e^-) applied to remove cations such as NH_4^+, Na^+, K^+, Mg^{2+}, and Ca^{2+} at constant voltages of 0.1 or 0.3 V, was calculated as

$$C_e = \frac{\int_0^t I dt}{F} \tag{3}$$

where t is the time for treatment (200 s), I is the applied current (A), and F is Faraday's constant (96 485 C mol^{-1}). The inefficiency of the charge consumed was calculated by subtracting the cations removed from the total charge passed through the circuit. Unlike the term charge efficiency (Λ; %), defined as the ratio of salt adsorption over charge transfer in an electrochemical system, which has been reported in some previous CDI and BDI studies,[48,49] the use of the cumulative

charge (or charge) was used here as this term compared both the efficiency (%) and total amount of charge (μmol e^-) used in the system at the same time.

Energy consumption (E_C, kW h per kg-N) in each stage was calculated as

$$E_C = \frac{\int_0^t VI dt}{C_N} \tag{4}$$

where V is the potential and C_N is the amount of NH_4^+ removed (kg-N). The energy for pumping energy was not included in this calculation.

Nitrogen recovery (R_N, %) was calculated as

$$R_N = \frac{C_{A,F} - C_{A,I}}{C_{A,I}} \times 100 \tag{5}$$

where $C_{A,I}$ is the initial concentration and $C_{A,F}$ is the final concentration (effluent concentration of the last stage) of NH_4^+.

The thermodynamic energy efficiency (TEE, %) was calculated as

$$TEE = \frac{\Delta g}{E_C} \times 100 \tag{6}$$

The specific Gibbs free energy of separation, Δg (J L^{-1}), was calculated as[50]

$$\Delta g = 2RT_a \left\{ \frac{C_{A,F}}{\gamma} \ln\left[\frac{C_{A,F} - \gamma C_{A,I}}{C_{A,F}(1-\gamma)}\right] - C_{A,I} \ln\left[\frac{C_{A,F} - \gamma C_{A,I}}{C_{A,I}(1-\gamma)}\right] \right\} \tag{7}$$

where R (8.314 J K^{-1} mol^{-1}) is the ideal gas constant, T_a (assumed to be 298 K) is the absolute temperature, and γ (0.5) is the water recovery.

2.5. Synthetic wastewater tests

Synthetic wastewater was prepared with NaCl (7 mM), NH_4Cl (5 mM), KCl (0.5 mM), $MgCl_2$ (1 mM), and $CaCl_2$ (1 mM) based on the measured cation concentrations in primary clarifier effluent from the Pennsylvania State University Waste Water Treatment Plant.[35] The tests were conducted at the same operating conditions described above for the ammonium enrichment and removal tests. The NH_4^+ concentration was measured using a discrete analyzer (SEAL analytical, AQ2), and the Na^+, K^+, Mg^{2+}, and Ca^{2+} concentrations were measured using inductively coupled plasma atomic emission spectrometry (Thermo Fisher Scientific, XSERIES 2). The solution used for tests in a successive stage was a freshly made solution based on the concentration of ions in the effluent from the previous stage.

3. Results and discussion

3.1. Ammonium enrichment from synthetic ammonium/sodium solution

3.1.1. Stepwise ammonium enrichment. In the first treatment stage (S1), there was a greater extent of water

1652 | Environ. Sci.: Water Res. Technol., 2020, 6, 1649–1657

This journal is © The Royal Society of Chemistry 2020

desalination at 0.3 V than at 0.1 V, as shown by the larger decrease in conductivity of the treated stream (Fig. 2b) and a higher conductivity of the concentrated stream. At a constant applied voltage (0.3 V), the conductivity changes in the second (S2) and third stage (S3) were slightly less than that obtained for the first stage (S1), based on the changes in conductivity normalized to the influent conductivity to each stage.

When the concentrated solution from the first stage (S1-C) was passed into the second stage, and then the effluent from that stage (S2-C) was used in the third stage, there was an overall 5-fold increase in the NH_4^+ concentration, from 5 mM to 25 mM, without appreciable changes in the concentration of Na^+ (Fig. 2c). The influent NH_4^+ concentration increased from 5 mM to 10 mM in the first stage (S1), 17 mM in the second stage concentrated effluent (S2), to the final concentration of 25 mM (S3). Throughout the same three stages, the Na^+ concentration changed by less than 7% due to its lower affinity for intercalation into the electrodes as well as the de-intercalation or exchange of ions during the stabilization step (Fig. S3b, d, and f†).

When a lower voltage of 0.1 V was applied, less ammonia was removed and therefore NH_4^+ was only concentrated by 53% rather than by 100% in the first stage (Fig. S3a and b†). Although NH_4^+ in the following two stages was <36%, NH_4^+ was more concentrated at even at the lower applied voltage of 0.1 V due to its higher initial concentration in the second (10 mM) and third (17 mM) stages compared to the first stage (5 mM) (Fig. S3c–f†). Based on these results, a higher fixed voltage of 0.3 V was chosen as a working voltage for the subsequent three-stage tests.

3.1.2 Selective ammonium enrichment and removal. The selectivity factors for NH_4^+ relative to that of Na^+ ranged from 20 to 103 for the first and third stages at an applied voltage of 0.1 V (Fig. 3a). At a higher fixed voltage of 0.3 V, these selectivity ratios were lower (range of 3 to 29) over the three stages due to the lack of sufficient NH_4^+, since Na^+ ions were removed when the concentration of the NH_4^+ ions was very low (Fig. S3a, c, and e†). For example, in the first stage after

removal of 100% of NH_4^+ at the higher applied voltage of 0.3 V there was Na^+ ion removal, resulting in 35 ± 3% of Na^+ removal (Fig. S3a†). However, since there was only 62 ± 5% of NH_4^+ removed at the lower applied voltage of 0.1 V, there was very little Na^+ removal (4 ± 1%). The relatively large range of the NH_4^+/Na^+ selectivity observed here (Fig. S3†) at 0.1 V was attributed to the relatively small amount of Na^+ removed (<0.6%). This small removal of Na^+ with a range from 0.2% (0.04 mM) to 0.6% (0.13 mM) resulted in the NH_4^+/Na^+ selectivity from 46 to 160.

As the NH_4^+ concentration was increased in each stage, the greater selectivity for NH_4^+ resulted in a different trend in the removal of the cations, with the moles of removed cations increasing with each stage for NH_4^+, and fewer Na^+ ions removed in the successive stage, regardless of applied voltage (Fig. 3b). In the first stage, the charge of 7 µmol e^- (0.1 V) was used to remove 3 µmol of NH_4^+, whereas <1 µmol of Na^+ was removed at the same time (Fig. S4a†). By the third stage, when a charge of 20 µmol e^- (0.3 V) was passed through the circuit, 11 µmol of NH_4^+ was removed compared to <1 µmol of Na^+.

3.1.3. Energy consumption and ammonium recovery. Less energy was always needed in the next stage compared to that required in the previous stage mainly due to the higher concentrations of NH_4^+ ions (Fig. 4a). The energy consumption for stage 1 was 1.0 kW h per kg-N (S1), decreasing to 0.6 kW h per kg-N in stage 2 (S2), and 0.4 kW h per kg-N in stage 3 (S3). This decreased energy was consistent with an increase in the NH_4^+ concentration from 5 mM in stage 1, to 7 mM in stage 2 and 8 mM in stage 3. Thus, the cumulative energy use for the three-stage process (from S1 to S3) to concentrate NH_4^+ by 5 times, from 5 to 25 mM, was 2.1 kW h per kg-N (Fig. 4b).

3.2. Ammonium enrichment from synthetic wastewater

The use of the three stage BDI process with synthetic wastewater enabled NH_4^+ enrichment of more than 6 times, from 5 mM to 32 mM, which was significantly higher than
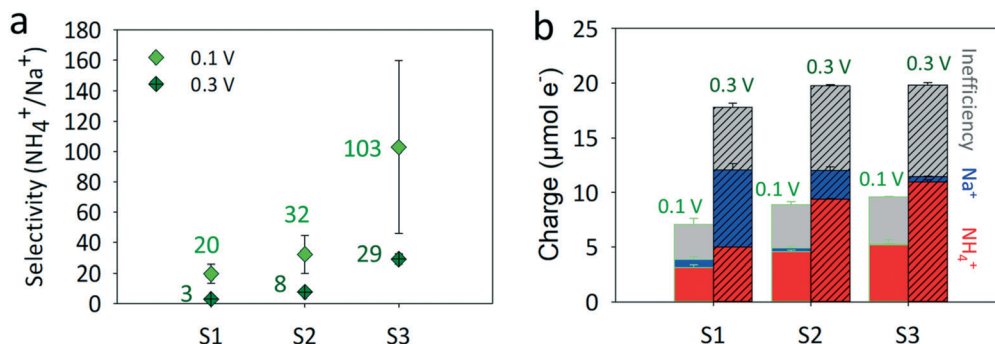

Fig. 3 (a) Selectivity of ions (NH_4^+/Na^+) over stages. (b) Amount of charges consumed to remove NH_4^+ (red) or Na^+ (blue) at constant voltages of 0.1 (plain bar) or 0.3 V (hatched bar). Inefficiency (grey) was calculated by the cumulative charges applied minus cation removed. Detailed data of removed cations (µmol) as a function of the amount of charge (µmol e^-) can be found in Fig. S4.† Concentration of the feed waters was varied depending on the effluent concentration of the previous stage (S1: 20 mM NaCl and 5 mM NH_4Cl, S2: 21 mM NaCl and 10 mM NH_4Cl, and S3: 21 mM NaCl and 17 mM NH_4Cl).

This journal is © The Royal Society of Chemistry 2020

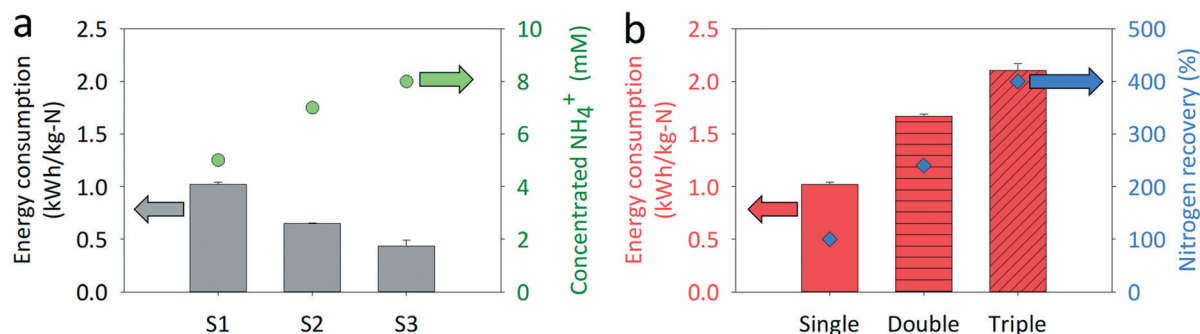Environ. Sci.: Water Res. Technol., 2020, 6, 1649–1657 | 1653

Fig. 4 Energy consumption (kW h per kg-N) of (a) each cell or (b) staged cell at a constant applied voltage of 0.3 V. Energy consumption of triple is the sum of S1, S2, and S3. (a) The amount of the concentrated NH_4^+ by each cell and (b) nitrogen recovery of the staged cell was calculated by dividing the NH_4^+ concentration of the effluent in each mode by 5 mM, the initial concentration of ammonium in the first stage (S1).

that of the sum of the other cations (Na^+, K^+, Mg^{2+}, and Ca^{2+}) (Fig. 5 and S5†). This indicated that the BDI still had a high selectivity for NH_4^+ over the bulk of the other cations present in the wastewater. The high selectivity of NH_4^+ is in line with previous findings that intercalation reactions of CuHCF to NH_4^+ are favorable over other cations present in

Fig. 5 Concentration of the feed, treated, and concentrated waters over (a) S1, (b) S2, and (c) S3 at an applied voltage of 0.3 V using synthetic wastewater.

wastewater when a mid-point potential of ~0.8 V was used.[35]

Based on the percentage in ion concentration over three stages, the CuHCF electrode showed enhanced selectivity for some ions, such as K^+ (218%, from 0.5 mM to 1.1 mM) and Ca^{2+} (171%, from 1.0 mM to 1.7 mM) relative to Na^+ (113%, from 7.0 mM to 8.0 mM) (Fig. 5). A particularly low selectivity (<15%) was found for Mg^{2+} among the cations tested throughout the three stages. The cation concentrations of the treated streams also showed the same trends as that of the concentrated streams. Thus, it can be seen that the cation selectivity of the CuHCF electrode in the BDI was in the order $NH_4^+ \gg K^+/Ca^{2+} > Na^+ \gg Mg^{2+}$, which was mostly followed the order of the Stokes or hydrated radius of the cations.[38]

Most of the charge consumed through the BDI was used to remove and recover NH_4^+ because of its high selectivity for NH_4^+, even when synthetic wastewater containing other cations was used as the influent (Fig. 6a). As the NH_4^+ concentration was increased, a greater proportion of the charge was used to remove NH_4^+ ions. For example, in the first stage, 18 µmol e^- was used to recover 5 µmol of NH_4^+, whereas <2 µmol of each of the other cations was removed at the same time. By the third stage, when a charge of 23 µmol e^- was passed through the circuit, 13 µmol of NH_4^+ was recovered compared to only <1 µmol of each of other cations. Throughout the experiments, charge inefficiencies were ~50% (Fig. 3b and 6a). Increasing solution conductivity (S1 in Fig. 6a versus S1 0.3 V in Fig. 3b) or the applied voltage (Fig. 3b) only slightly increased the charge efficiency of the system. Greater improvement in the charge efficiency will therefore require electrodes that can contain additional CuHCF catalyst and thus more active sites to further enhance the overall energy efficiency of the BDI system. In addition, this approach of improving the charge efficiency could also enhance the present energy efficiency (the thermodynamic minimum energy divided by energy demand of the system) of 5.7 ± 1.1% calculated for all experiments when a fixed applied voltage of 0.3 V.

As more nitrogen was recovered in each stage, less energy was required (Fig. 6b). In the staged mode, the energy consumption of 1.0 kW h per kg-N (single; S1), 1.7 kW h per
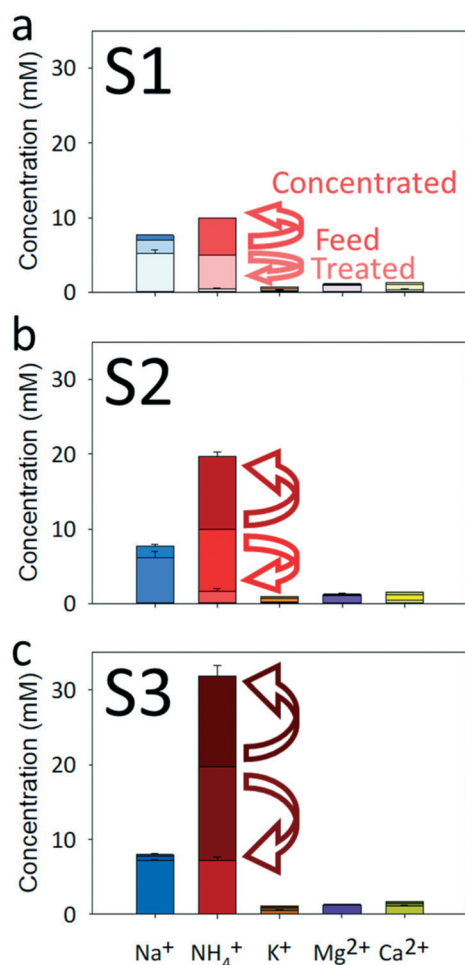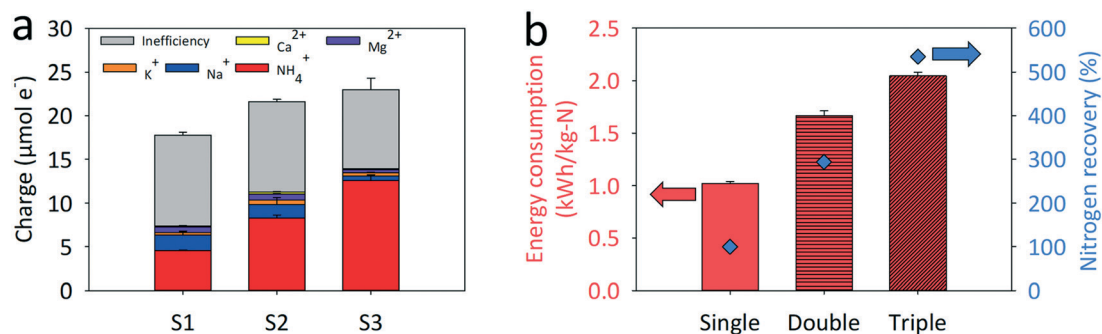
Fig. 6 (a) Amount of charges consumed to remove cations present in synthetic wastewater at constant voltages of 0.3 V. (b) Energy consumption (kW h per kg-N) and nitrogen recovery (%) of staged cell at a constant applied voltage of 0.3 V using synthetic wastewater. Energy consumption of triple is the sum of S1, S2, and S3.

kg-N (double; S1 + S2), and 2.0 kW h per kg-N (triple; S1 + S2 + S3) was calculated, indicating that the energy used in the second (0.7 kW h per kg-N) and third (0.3 kW h per kg-N) stages were lower than that of the first stage (1.0 kW h per kg-N). This energy was lowered in each stage, due to the increased nitrogen recovery of 100% in the first stage, 294% with two stages, and 535% with three stages, resulting in a cumulative energy consumption of only 2.0 kW h per kg-N to concentrate NH_4^+ by >6 times from 5 mM to 32 mM.

3.3. Implications for wastewater treatment

The energy used by the three-stage BDI system to concentrate NH_4^+ from 5 to 32 mM (nitrogen recovery of 535%) was only 2.0 kW h per kg-N using a synthetic wastewater as a feed (Fig. 6b). This was less than that needed for other electrochemical processes, for example 4.4–21.7 kW h per kg-N for CDI (initial NH_4^+ of ~3 mM),[29–31] 8.5 kW h per kg-N for ED (initial nitrogen of 286 mM),[17] and 126–622 kW h per kg-N for electro-oxidation (EO, initial NH_4^+ of ~4 mM or ~8 mM).[51,52] For all of these processes additional treatment would be needed to purify and recover the ammonium, such as air stripping followed by an ammonia scrubber, and then subsequent production of the fertilizer such as $(NH_4)_2SO_4$.[16–18] The energy consumption for conventional air stripping and a scrubber is relatively high (~6–9 kW h per kg-N).[16,53] Thus, to increase the overall efficiency of the process to purify and recover ammonium, it is important to use more concentrated streams of ammonium than the original effluent as there is minimum energy consumption of the subsequent process. Hybrid biological-electrochemical processes, such as microbial electrolysis cells, can be operated to directly extract NH_3-N from a membrane-coated porous metal cathode, with 1.6–2.5 kW h per kg-N of energy consumption.[54,55] While conventional biological processes based on nitrification and denitrification can remove ammonia at an energy consumption (1.7 kW h per kg-N) similar to BDI,[10] the conversion of ammonia to nitrogen gas wastes the energy in the ammonia. For example, ammonia concentrations of 2–5 mM (28 to 70 mg L^{-1}) are equivalent to 0.39–0.98 kW h m^{-3} to produce that amount of ammonia by

the Haber Bosch process (assuming 14 kW h per kg-N), which is 65–160% of the energy needed to treat conventional wastewaters of 0.6 kW h m^{-3}. Thus, the use of electrochemical cells with selective battery electrodes connected in series could represent an effective method for ammonium enrichment and recovery due to its ability to achieve high nitrogen recovery rate (540%) with relatively low energy consumption (2.0 kW h per kg-N), especially considering the high energy demands for producing ammonia using the Haber Bosch process. Although the previous tests with actual wastewaters using a BDI cell have shown that there is no appreciable difference in performance between synthetic and actual wastewaters, as residual organic matter did not impact cation removal,[35] tests using actual wastewater with a three-stage BDI system will further help to demonstrate its feasibility compared to other processes in practical applications.

4. Conclusions

A three-stage BDI system with CuHCF electrodes was developed and tested to selectively remove and concentrate ammonium derived from a wastewaters. Ammonium was concentrated greater than 6 times, from 5 to 32 mM (90 to 576 mg L^{-1}), with minimal changes (<1 mM) in the concentration of other competing cations (Na^+, K^+, Mg^{2+}, and Ca^{2+}) present in the water, indicating a high ammonium ion selectivity using the CuHCF electrodes. The energy used by the three-stage BDI system to concentrate NH_4^+ from 5 to 32 mM was only 2.0 kW h per kg-N, which was less than that needed for other electrochemical processes such as CDI, ED, or EO processes. Thus, the use of the staged BDI system provided an energy-efficient approach due to the great selectivity of ammonium at the low energy demand of the system. The development of an automated BDI system with an adjustable flow rate will be needed to further improvements in overall selectivity and energy demands.

Conflicts of interest

There are no conflicts to declare.

Acknowledgements

References

1   J. N. Galloway, A. R. Townsend, J. W. Erisman, M. Bekunda, Z. Cai, J. R. Freney, L. A. Martinelli, S. P. Seitzinger and M. A. Sutton, Transformation of the nitrogen cycle: Recent trends, questions, and potential solutions, *Science*, 2008, **320**, 889–892.

2   G. F. McIsaac, M. B. David, G. Z. Gertner and D. A. Goolsby, Nitrate flux in the Mississippi River, *Nature*, 2001, **414**, 166–167.

3   J. H. Ryther and W. M. Dunstan, Nitrogen, phosphorus, and eutrophication in the coastal marine environment, *Science*, 1971, **171**, 1008–1013.

4   D. J. Conley, H. W. Paerl, R. W. Howarth, D. F. Boesch, S. P. Seitzinger, K. E. Havens, C. Lancelot and G. E. Likens, Controlling eutrophication: Nitrogen and phosphorus, *Science*, 2009, **323**, 1014–1015.

5   R. D. Cusick, Y. Kim and B. E. Logan, Energy capture from thermolytic solutions in microbial reverse-electrodialysis cells, *Science*, 2012, **335**, 1474–1477.

6   C. A. Kinney, E. T. Furlong, S. D. Zaugg, M. R. Burkhardt, S. L. Werner, J. D. Cahill and G. R. Jorgensen, Survey of organic wastewater contaminants in biosolids destined for land application, *Environ. Sci. Technol.*, 2006, **40**, 7207–7215.

7   P. K. Cornejo, Q. Zhang and J. R. Mihelcic, How does scale of implementation impact the environmental sustainability of wastewater treatment integrated with resource recovery?, *Environ. Sci. Technol.*, 2016, **50**, 6680–6689.

8   P. Ledezma, J. Jermakka, J. Keller and S. Freguia, Recovering nitrogen as a solid without chemical dosing: Bio-electroconcentration for recovery of nutrients from urine, *Environ. Sci. Technol. Lett.*, 2017, **4**, 119–124.

9   M. Qin, Y. Liu, S. Luo, R. Qiao and Z. He, Integrated experimental and modeling evaluation of energy consumption for ammonia recovery in bioelectrochemical systems, *Chem. Eng. J.*, 2017, **327**, 924–931.

10 S. Lackner, E. M. Gilbert, S. E. Vlaeminck, A. Joss, H. Horn and M. C. M. van Loosdrecht, Full-scale partial nitritation/anammox experiences – An application survey, *Water Res.*, 2014, **55**, 292–303.

11 A. Joss, D. Salzgeber, J. Eugster, R. König, K. Rottermann, S. Burger, P. Fabijan, S. Leumann, J. Mohn and H. Siegrist, Full-scale nitrogen removal from digester liquid with partial nitritation and anammox in one SBR, *Environ. Sci. Technol.*, 2009, **43**, 5301–5306.

12 P. L. McCarty, J. Bae and J. Kim, Domestic Wastewater Treatment as a Net Energy Producer–Can This be Achieved?, *Environ. Sci. Technol.*, 2011, **45**, 7100–7106.

13 L. Pal, B. Kraigher, B. Brajer-Humar, M. Levstek and I. Mandic-Mulec, Total bacterial and ammonia-oxidizer community structure in moving bed biofilm reactors treating municipal wastewater and inorganic synthetic wastewater, *Bioresour. Technol.*, 2012, **110**, 135–143.

14 J. L. Shore, W. S. M'Coy, C. K. Gunsch and M. A. Deshusses, Application of a moving bed biofilm reactor for tertiary ammonia treatment in high temperature industrial wastewater, *Bioresour. Technol.*, 2012, **112**, 51–60.

15 S. Wang, Y. Peng, B. Ma, S. Wang and G. Zhu, Anaerobic ammonium oxidation in traditional municipal wastewater treatment plants with low-strength ammonium loading: Widespread but overlooked, *Water Res.*, 2015, **84**, 66–75.

16 M. A. Boehler, A. Heisele, A. Seyfried, M. Grömping and H. Siegrist, $(NH_4)_2SO_4$ recovery from liquid side streams, *Environ. Sci. Pollut. Res.*, 2015, **22**, 7295–7305.

17 W. A. Tarpeh, J. M. Barazesh, T. Y. Cath and K. L. Nelson, Electrochemical stripping to recover nitrogen from source-separated urine, *Environ. Sci. Technol.*, 2018, **52**, 1453–1460.

18 P. Liao, A. Chen and K. Lo, Removal of nitrogen from swine manure wastewaters by ammonia stripping, *Bioresour. Technol.*, 1995, **54**, 17–20.

19 Z. Wang, H. Gong, Y. Zhang, P. Liang and K. Wang, Nitrogen recovery from low-strength wastewater by combined membrane capacitive deionization (MCDI) and ion exchange (IE) process, *Chem. Eng. J.*, 2017, **316**, 1–6.

20 A. T. Williams, D. H. Zitomer and B. K. Mayer, Ion exchange-precipitation for nutrient recovery from dilute wastewater, *Environ. Sci.: Water Res. Technol.*, 2015, **1**, 832–838.

21 W. Xue, K. Yamamoto and T. Tobino, Membrane fouling and long-term performance of seawater-driven forward osmosis for enrichment of nutrients in treated municipal wastewater, *J. Membr. Sci.*, 2016, **499**, 555–562.

22 O. Kavvada, W. A. Tarpeh, A. Horvath and K. L. Nelson, Life-cycle cost and environmental assessment of decentralized nitrogen recovery using ion exchange from source-separated urine through spatial modeling, *Environ. Sci. Technol.*, 2017, **51**, 12061–12071.

23 S. Lee and R. M. Lueptow, Toward a reverse osmosis membrane system for recycling space mission wastewater, *Life Support Biosphere Sci.*, 2000, **7**, 251–261.

24 Y. Wimalasiri, M. Mossad and L. Zou, Thermodynamics and kinetics of adsorption of ammonium ions by graphene laminate electrodes in capacitive deionization, *Desalination*, 2015, **357**, 178–188.

25 K. Fang, H. Gong, W. He, F. Peng, C. He and K. Wang, Recovering ammonia from municipal wastewater by flow-electrode capacitive deionization, *Chem. Eng. J.*, 2018, **348**, 301–309.

26 P. Xu, J. E. Drewes, D. Heil and G. Wang, Treatment of brackish produced water using carbon aerogel-based capacitive deionization technology, *Water Res.*, 2008, **42**, 2605–2617.

27 C. Huyskens, J. Helsen and A. B. de Haan, Capacitive deionization for water treatment: Screening of key performance parameters and comparison of performance for different ions, *Desalination*, 2013, **328**, 8–16.

1656 | *Environ. Sci.: Water Res. Technol.*, 2020, **6**, 1649–1657

This journal is © The Royal Society of Chemistry 2020

28　C. Zhang, J. Ma and T. D. Waite, The impact of absorbents on ammonia recovery in a capacitive membrane stripping system, *Chem. Eng. J.*, 2020, **382**, 122851.

29　R. Broséus, J. Cigana, B. Barbeau, C. Daines-Martinez and H. Suty, Removal of total dissolved solids, nitrates and ammonium ions from drinking water using charge-barrier capacitive deionisation, *Desalination*, 2009, **249**, 217–223.

30　C. Zhang, J. Ma, J. Song, C. He and T. D. Waite, Continuous ammonia recovery from wastewaters using an integrated capacitive flow electrode membrane stripping system, *Environ. Sci. Technol.*, 2018, **52**, 14275–14285.

31　C. Zhang, J. Ma, D. He and T. D. Waite, Capacitive membrane stripping for ammonia recovery (CapAmm) from dilute wastewaters, *Environ. Sci. Technol. Lett.*, 2018, **5**, 43–49.

32　K. C. Smith and R. Dmello, Na-ion desalination (NID) enabled by Na-blocking membranes and symmetric Na-intercalation: porous-electrode modeling, *J. Electrochem. Soc.*, 2016, **163**, A530–A539.

33　K. C. Smith, Theoretical evaluation of electrochemical cell architectures using cation intercalation electrodes for desalination, *Electrochim. Acta*, 2017, **230**, 333–341.

34　S. Liu and K. C. Smith, Quantifying the trade-offs between energy consumption and salt removal rate in membrane-free cation intercalation desalination, *Electrochim. Acta*, 2018, **271**, 652–665.

35　T. Kim, C. A. Gorski and B. E. Logan, Ammonium removal from domestic wastewater using selective battery electrodes, *Environ. Sci. Technol. Lett.*, 2018, **5**, 578–583.

36　D.-H. Nam and K.-S. Choi, Bismuth as a new chloride-storage electrode enabling the construction of a practical high capacity desalination battery, *J. Am. Chem. Soc.*, 2017, **139**, 11055–11063.

37　R. Y. Wang, B. Shyam, K. H. Stone, J. N. Weker, M. Pasta, H. W. Lee, M. F. Toney and Y. Cui, Reversible multivalent (monovalent, divalent, trivalent) ion insertion in open framework materials, *Adv. Energy Mater.*, 2015, **5**, 1401869.

38　G. M. Geise, D. R. Paul and B. D. Freeman, Fundamental water and salt transport properties of polymeric materials, *Prog. Polym. Sci.*, 2014, **39**, 1–42.

39　C. D. Wessells, S. V. Peddada, M. T. McDowell, R. A. Huggins and Y. Cui, The effect of insertion species on nanostructured open framework hexacyanoferrate battery electrodes, *J. Electrochem. Soc.*, 2011, **159**, A98–A103.

40　K. Itaya, T. Ataka and S. Toshima, Spectroelectrochemistry and electrochemical preparation method of Prussian blue modified electrodes, *J. Am. Chem. Soc.*, 1982, **104**, 4767–4772.

41　F. Scholz and A. Dostal, The formal potentials of solid metal hexacyanometalates, *Angew. Chem., Int. Ed. Engl.*, 1996, **34**, 2685–2687.

42　G. El Diwani, S. El Rafie, N. N. El Ibiari and H. I. El-Aila, Recovery of ammonia nitrogen from industrial wastewater treatment as struvite slow releasing fertilizer, *Desalination*, 2007, **214**, 200–214.

43　J. D. Doyle and S. A. Parsons, Struvite formation, control and recovery, *Water Res.*, 2002, **36**, 3925–3940.

44　E. V. Münch and K. Barr, Controlled struvite crystallisation for removing phosphorus from anaerobic digester sidestreams, *Water Res.*, 2001, **35**, 151–159.

45　T. Kim, C. A. Gorski and B. E. Logan, Low energy desalination using battery electrode deionization, *Environ. Sci. Technol. Lett.*, 2017, **4**, 444–449.

46　C. D. Wessells, R. A. Huggins and Y. Cui, Copper hexacyanoferrate battery electrodes with long cycle life and high power, *Nat. Commun.*, 2011, **2**, 550.

47　T. Kim, B. E. Logan and C. A. Gorski, High power densities created from salinity differences by combining electrode and Donnan potentials in a concentration flow cell, *Energy Environ. Sci.*, 2017, **10**, 1003–1012.

48　T. Kim, J. E. Dykstra, S. Porada, A. van der Wal, J. Yoon and P. M. Biesheuvel, Enhanced charge efficiency and reduced energy use in capacitive deionization by increasing the discharge voltage, *J. Colloid Interface Sci.*, 2015, **446**, 317–326.

49　M. Son, V. Pothanamkandathil, W. Yang, J. S. Vrouwenvelder, C. A. Gorski and B. E. Logan, Improving the thermodynamic energy efficiency of battery electrode deionization using flow-through electrodes, *Environ. Sci. Technol.*, 2020, **54**, 3628–3635.

50　L. Wang, J. E. Dykstra and S. Lin, Energy efficiency of capacitive deionization, *Environ. Sci. Technol.*, 2019, **53**, 3366–3378.

51　C. Zhang, D. He, J. Ma and T. D. Waite, Active chlorine mediated ammonia oxidation revisited: Reaction mechanism, kinetic modelling and implications, *Water Res.*, 2018, **145**, 220–230.

52　D. Sun, X. Hong, K. Wu, K. S. Hui, Y. Du and K. N. Hui, Simultaneous removal of ammonia and phosphate by electro-oxidation and electrocoagulation using RuO2–IrO2/Ti and microscale zero-valent iron composite electrode, *Water Res.*, 2020, **169**, 115239.

53　J. Desloover, A. Abate Woldeyohannis, W. Verstraete, N. Boon and K. Rabaey, Electrochemical resource recovery from digestate to prevent ammonia toxicity during anaerobic digestion, *Environ. Sci. Technol.*, 2012, **46**, 12209–12216.

54　D. Hou, A. Iddya, X. Chen, M. Wang, W. Zhang, Y. Ding, D. Jassby and Z. J. Ren, Nickel-based membrane electrodes enable high-rate electrochemical ammonia recovery, *Environ. Sci. Technol.*, 2018, **52**, 8930–8938.

55　P. Kuntke, P. Zamora, M. Saakes, C. J. N. Buisman and H. V. M. Hamelers, Gas-permeable hydrophobic tubular membranes for ammonia recovery in bio-electrochemical systems, *Environ. Sci.: Water Res. Technol.*, 2016, **2**, 261–265.